Polymer Chemistry

PAPER

View Article Online
View Journal | View Issue

Cite this: *Polym. Chem.*, 2017, **8**, 6981

A novel self-healing electrochromic film based on a triphenylamine cross-linked polymer†

Rongzong Zheng,[a] Jiaqiang Zhang,[b] Chunyang Jia, *[a] Zhongquan Wan,[a] Yaru Fan,[a] Xiaolong Weng,[a] Jianliang Xie[a] and Longjiang Deng[a]

Received 24th August 2017,
Accepted 18th October 2017

DOI: 10.1039/c7py01434a

rsc.li/polymers

The cracking of electrochromic materials due to aging or reiterative bending is a major problem which noticeably degrades the performance of electrochromic devices. In the present research, we successfully induced a triphenylamine derivative into furfuryl glycidyl ether, and further by a DA cross-linking polymerization reaction with maleimide (MA) to yield polymer DATPFMA. The color of the polymer film could be switched from faint yellow to green grey to dark blue. The observed coloration efficiency values of the polymer for the electrochromic process were 82.2 and 175.3 $cm^2\ C^{-1}$ at 580 and 1060 nm, and the coloring and bleaching response times were 4.1 and 11.0 s, respectively. The self-healing process of the polymer film at 110 °C was observed by optical microscopy and the self-healing rate was about 80%. The results indicate that the polymer DATPFMA is a novel electrochromic material with noteworthy self-healing properties.

Introduction

Electrochromic materials have attracted great interest from material scientists and engineers due to the reversible optical change in absorption or transmittance induced by external voltages.[1] Currently, inorganic transition metal oxides,[2] organic small molecular materials[3] and π-conjugated polymers[4] are some of the most widely used species of electrochromic materials. Recently, organic electrochromic materials have gained special attention from researchers and design engineers due to their structural modification[5] and tunable color response.[6] Triphenylamine (TPA), an important organic electrochromic material, has the characteristic structure of the electroactive site of the nitrogen center, which has three adjacent electron-donor phenyl groups with a propeller-like geometry. Compared with π-conjugated TPA-based polymers, non-conjugated TPA-based derivatives are optically transmissive in the neutral state and exhibit variable colors in the oxidized state with high contrast. In essence, non-conjugated TPA-based polymers are more soluble, and the electrochemical oxidation behavior is more stable and the electrochromic reversibility is better than conjugated TPA-based polymers, and their anodic oxidation behavior has been well studied.[7] Recently, our group also reported several TPA derivatives and obtained some important results,[8] and non-conjugated TPA-based derivatives are excellent performance materials for electrochromism.[9]

In the last few decades, the research efforts on electrochromism have been mainly focused on some prime performance parameters like contrast ratio,[10] response time[11] and active life stability.[12] Recently, more research studies have been carried out in optoelectronics for the fabrication of flexible,[13] stretchable[14] and even wearable electronic devices.[15] Despite their noteworthy properties, electrochromic devices (ECDs) are still facing challenges like the appearance of cracks in the electrochromic material with passage of time due to reiterative bending. These issues strongly degrade the performance of electrochromic materials and hence limit the overall efficiency and active life of ECDs.

Materials with a self-healing ability are particularly attractive in the field of smart materials because these materials[16] have the intrinsic capacity to repair the cracks to obviate such risks, thereby leading to reduced waste, improved lifetime, durability and reliability of the devices. It is believed that the use of an electrochromic polymer film with self-healing properties would be an effective approach to overcome the risk of the scar generation in ECDs. Until now, self-healing polymers based on the Diels–Alder (DA) reaction, which is an effective method for the implementation of intrinsic self-healing into functional materials, have been deeply studied for various electronic and optoelectronic applications like conducting films,[17] OLEDs,[18] supercapacitors[14,19] *etc*.

In this paper, a novel polymer DATPFMA, which has electrochromic and self-healing properties, was synthesized and

[a]*State Key Laboratory of Electronic Thin Films and Integrated Devices, National Engineering Research Center of Electromagnetic Radiation Control Materials, School of Microelectronics and Solid-State Electronics, University of Electronic Science and Technology of China, Chengdu 610054, PR China. E-mail: cyjia@uestc.edu.cn; Fax: +86 28 83202569; Tel: +86 28 83201991*

[b]*Beijing Spacecrafts, China Academy of Space Technology, Beijing 100190, PR China*

†Electronic supplementary information (ESI) available. See DOI: 10.1039/c7py01434a

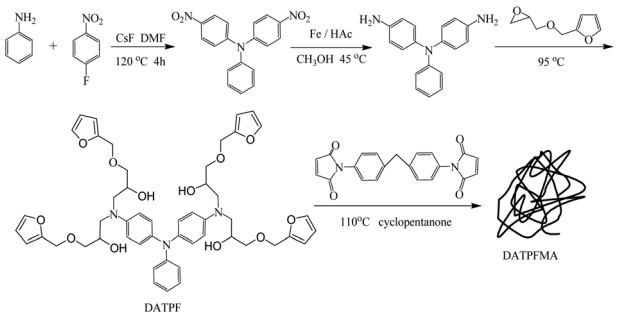

Scheme 1 The synthetic route of the polymer DATPFMA.

reported. As described in Scheme 1, the TPA derivative was the electrochromic unit and was induced into the furfuryl glycidyl ether (FGE), and further by a DA cross-linking polymerization reaction with maleimide (MA) to obtain the non-conjugated TPA-based polymer DATPFMA. It not only exhibits electrochromic properties but also possesses self-healing nature, which indicates that DATPFMA is a promising material to overcome the cracking problems in ECDs.

Experimental section

Experimental reagents

A ITO (15 Ω cm^{-2}, commercially purchased) coated glass substrate was cut into pieces with a size of 0.8 cm × 4 cm, ultrasonically washed with acetone, ethanol, and deionized water for 15 minutes, sequentially, and then immersed in ethanol for use. 0.1 mol L^{-1} $LiClO_4$ in acetonitrile (CH_3CN) was employed as the electrolyte in the test. Other reagents and solvents were purchased from commercial sources and used without any further purification.

Instruments

Infrared spectra were recorded by FT-IR (8400s, Shimadzu), high resolution mass spectral (HRMS) data were determined with an FTICR-APEX instrument, nuclear magnetic resonance (NMR) spectra were obtained on a Brücker AM 400 NMR instrument, and the structural characterization was consistent with the target compounds. The average molecular weight of the polymer was tested by GPC (Waters 2414), using THF as the solvent and PS as the standard.

The electrochemical analysis of the polymer DATPFMA film, which was coated on the ITO glass substrate, was carried out by cyclicvoltammetry (CV) and electrochemical impedance spectroscopy (EIS) on a CHI660C electrochemical workstation in electrolyte solution, the reference electrode was Ag/AgCl in saturated KCl solution and Ti sheet was used as the counter electrode.

Optical properties and kinetic features of the polymer DATPFMA film were observed on a spectrophotometer (UV-2250, Shimadzu) and CHI660 electrochemical workstation. An *in situ* colorimeter (SP60, X-Rite) was used to test the chromaticity of the polymer film, which was switched to different states by the amperometric *i–t* method on the electrochemical workstation before tests; each state of the film was tested at least three times to approximate average values.

The surface morphology of the polymer DATPFMA film before and after electrochromism with several circulations was measured by using a scanning electron microscope (SEM, JEOL, JSM-7600F). Thermogravimetric analysis (TGA) was conducted on a WRT-1D (Beijing) with approximately 3–5 mg of samples heated under flowing nitrogen (flow rate: 35 cm^3 min^{-1}). Differential scanning calorimetry (DSC) analyses were carried out on a Q200 (TA, USA) at a heating rate of 10 °C min^{-1} under flowing nitrogen (flow rate: 50 cm^3 min^{-1}), and the enthalpy value (ΔH) was determined by using Universal Analysis 2000.

Synthesis

N-(4-Aminophenyl)-*N*-phenylbenzene-1,4-diamine (DATP) was synthesized according to the literature.[20]

The synthesis of DATPF. 6.25 g FGE (40.5 mmol) was heated up to 50 °C in a flask and stirred without any solvent under nitrogen protection, then 2.75 g DATP (10 mmol) and 0.1 g NaOH as the catalyst were added to the flask and the mixture was stirred at 90 °C for 6 h in an inert environment. After 6 h, the crude product was eluted through a silica-gel column with a dichloromethane and ethanol mixture (volume ratio was 1 : 1) to give light yellow colored DATPF, 7.45 g (89%). ^{1}H NMR (400 MHz, [D1]$CDCl_3$, 25 °C, TMS): δ = 7.41 (t, J = 6.8 Hz, 4H), 7.07 (t, J = 7.2 Hz, 2H), 6.72 (m, 1H), 6.54–6.05 (m, 18H), 4.68 (m, 8H), 4.53 (s, 8H), 3.80 (m, 4H), 3.57–3.68 (m, 8H). MS-ESI (*m*/*z*): calcd for ($C_{50}H_{57}N_3O_{12}$): 891.3316; found 892.3972 $[M + H]^+$.

The preparation of the polymer film. 6.9 g MA (18.8 mmol) and 4.2 g DATPF (4.7 mmol) were dissolved in 20 mL cyclopentanone, then the mixture was stirred at 110 °C for 4 h and the solvent was evaporated under vacuum to give a brownish yellow polymer. The obtained polymer powder was added into 50 mL methanol and kept stirring for 4 h under 50 °C several times for washing purposes until the methanol was clear and colorless, the purified polymer was obtained after drying. ^{1}H NMR (400 MHz, [D6]DMSO, 25 °C, TMS): 7.64 (t, J = 6.4 Hz, 8H), 7.62 (t, J = 1.6 Hz, 8H), 7.34 (t, J = 6.8 Hz, 1.55H), 6.68–6.47 (m, 6H), 6.42–6.05 (m, 18H), 5.02 (d, J = 2.0 Hz, 2.45H), 4.68 (m, 8H), 4.03–4.44 (m, 12H), 3.53–3.83 (m, 16H), 2.87–3.11 (m, 5H). ^{13}C NMR (400 MHz, [D6]DMSO, 25 °C, TMS): 178.1, 174.2, 151.6, 143.1, 137.7, 129.1, 110.4, 109.4, 90.5, 80.7, 72.1, 68.6, 67.2, 50.1, 43.4, 22.7. M_w was 22 700, PDI (M_w/M_n) was 1.28, and the cross-linking degree was calculated to be 61.4%.

The viscous polymer DATPFMA mixture (density: 1.15 g mL^{-1}, the solvent was cyclopentanone) was dropped onto a clean ITO glass substrate coated with 3M tape (thickness: 10 μm), using a plastic scraper to obtain homogeneous DATPFMA polymer films, and then dried at 110 °C for 6 h.

Results and discussion

Synthesis and characterization

The formation of DATPFMA was confirmed by FT-IR, compared with DATPF and MA, and the results are shown in Fig. 1.

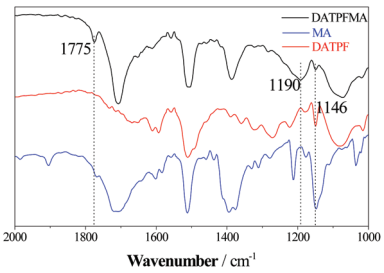

Fig. 1 The FT-IR spectra of DATPFMA, DATPF and MA.

The peaks which appeared clearly at 1775 and 1190 cm^{-1} in the spectra were ascribed to the stretching vibrations of the C=O bond as well as the asymmetric and symmetric stretching vibrations of the C–C bond,[21] which were specific to the DA adduct group. Meanwhile, the intensity of the peak at 1146 cm^{-1} in the DATPFMA spectrum is much lower than that of DATPF, which can be ascribed to the fact that the furan ring was consumed by MA.[22] All the differences indicate that DATPF and MA successfully cross-linked to give polymer DATPFMA.

The thermodynamic properties of the polymer DATPFMA were analyzed by DSC in the temperature range of 25–300 °C and are shown in Fig. 2a. The DATPF curve without obvious endothermic peaks indicates the thermodynamic stability of DATPF, and the MA curve exhibits two sharp endothermic peaks because of the crystal transfer and fusion. A broad endothermic peak lying between the temperature range of 100 to 160 °C represents the breakage of DA bonds in the molecular structure of the DATPFMA polymer.

In order to further investigate the thermodynamic stability of polymer DATPFMA, MA and DATPF, their corresponding TGA curves were obtained from room temperature to 800 °C (Fig. 2b). The curves show that MA and DATPF have two loss stages, while the polymer DATPFMA has three loss stages. An obvious weight loss has been observed at around 190 °C for DATPF, while MA shows remarkable stability and its weight loss stage starts at around 450 °C. The observed weight loss for DATPFMA, DATPF and MA in N_2 was about 10% at the corresponding temperature of 350 °C, 306 °C and 490 °C, respectively. The DTG curve of the polymer DATPFMA (Fig. 2c) indicates that DATPFMA is thermally decomposed in three steps, the first loss stage starts at 286.3 °C with 18.9% weight loss, and the second loss stage starts at 422.8 °C with 24.7% weight loss, and finally the maximum weight loss of about 50.3% was observed between 572.6 and 704.7 °C. The DATPFMA was completely decomposed and the residual weight was just about 6.5% at 720 °C. These results showed that the polymer DATPFMA has excellent thermodynamic stability, and can be used reliably and safely even at high temperature.

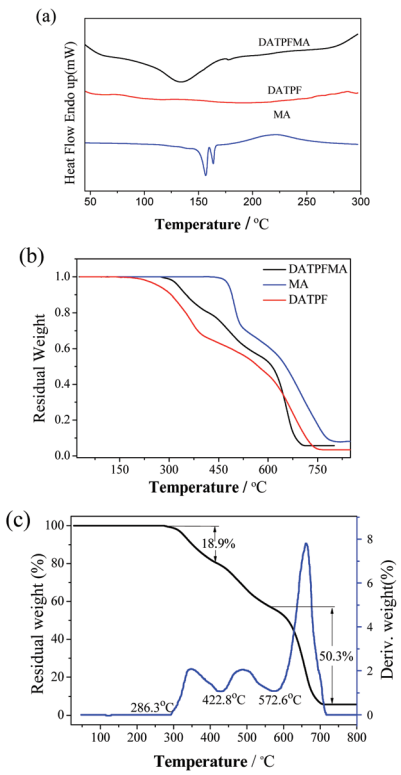

Fig. 2 (a) The DSC curves of DATPFMA, DATPF and MA. (b) The TG curves of DATPFMA, DATPF and MA. (c) The TGA curve and the DTG curve of DATPFMA.

Electrochromic properties

The polymer DATPFMA film was precoated on a ITO glass substrate (~8–10 μm), and its electrochemical behaviors were investigated by cyclic voltammetry (CV) in the range from 0 to 0.8 V. The CV curve of DATPFMA reveals redox peaks at E_{ox1} = 0.26 V, E_{ox2} = 0.35 V, E_{ox3} = 0.55 V, E_{red1} = 0.32 V, and E_{red2} = 0.51 V, respectively, as shown in Fig. 3a. The DATPFMA film displays variable colors from faint yellow to green grey to dark blue as the applied voltage varies from 0 V to 0.45 V and 0.7 V, respectively (Table 1).

The color of the DATPFMA film is evaluated by colorimetric analysis with the results of L^* (luminance), a^* (hue), and b^* (saturation). The L^*, a^*, and b^* parameters of the DATPFMA film and its images under different voltages of 0 V, 0.45 V, and 0.7 V are shown in Table 1.

The electrochromic behavior of DATPFMA can be explained by the fact that the TPA unit in the composite structure acts as an efficient electron donor and easily oxidized with the applied voltage. The electrochemical behavior and proposed inter-valence charge transfer[7] aspects of DATPFMA are shown in Scheme 2. The central nitrogen atom of the TPA group was taken an electron to be oxidized easily at a low applied voltage (0.26 V), and the stable mono-cation radical was named $DATPFMA^{1+}$. Similarly, when the applied voltage increased further oxidation occurred which formed $DATPFMA^{2+}$ in the second oxidation state and could be further oxidized to form $DATPFMA^{3+}$ when the applied voltage was increased up to 0.7 V. The absorbance spectral curves of the polymer DATPFMA film in different states and the different colorations were recorded and are shown in Fig. 3b. The sharp peak at

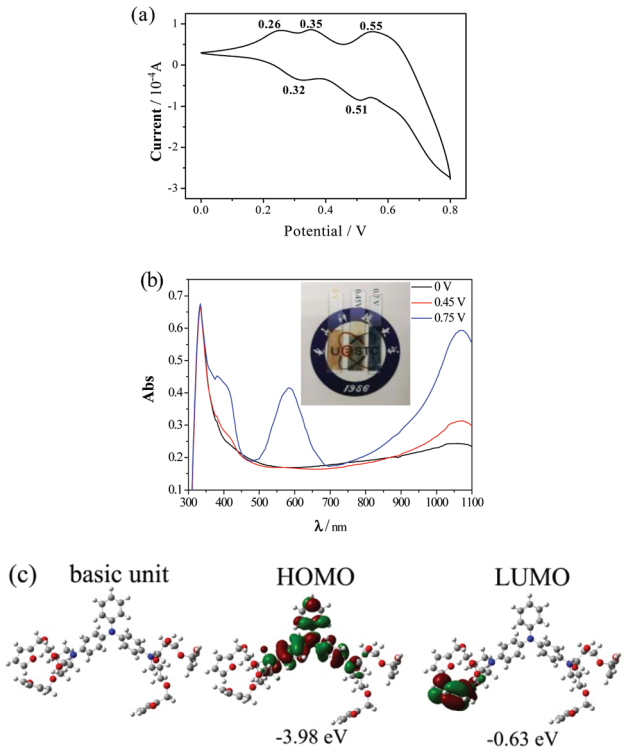

Fig. 3 (a) CV curve of the polymer DATPFMA film at 100 mV s^{-1} in 0.1 M $LiClO_4/CH_3CN$ solution, (b) UV-Vis absorption spectra of the polymer DATPFMA film under different voltages, and (c) the optimized geometries and frontier molecular orbitals of DATPF.

Table 1 Color parameters and optical images of the DATPFMA film

0 V		0.45 V		0.7 V	
Faint yellow		Green grey		Dark blue	
L^* 73.95 a^* +0.89 b^* +12.21		L^* 68.20 a^* −0.14 b^* +4.14		L^* 51.26 a^* −7.94 b^* −31.29	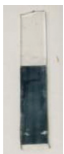

331 nm represents the π–π* transition of the aromatic phenyl ring of the TPA group.[7,23] It is clear that the absorbance of the polymer film changed at 385 nm, which indicates the increasing oxidation of the TPA group in the second oxidation stage. The broad absorption in the near infrared region (~1060 nm) can be explained on the basis of the inter-valence transfer between excitation states, in which positive charge is centered at different nitrogen atoms[7] (Scheme 2). Similarly, a new characteristic peak appears at 580 nm in the blue region of the visible spectra when the applied voltage was further increased to 0.7 V, which represents the existence of the third oxidation state.

The energy levels of the highest occupied molecular orbital (HOMO) and the lowest unoccupied molecular orbital (LUMO) of the monomer DATPF were also calculated to be −3.98 eV and −0.63 eV, respectively (Fig. 3c). And its band gap (E_g) is 3.35 eV, which was a little larger than other TPA-based polymers,[24] the main reason may be the fact that the TPA unit was not replaced with an electron-rich substituent group.

As shown in Fig. 4, the response time of the polymer DATPFMA film was calculated at the wavelengths of 580 and 1060 nm between 0 V (bleached) and 0.75 V (colored). The electrochromic film exhibits response times of 11.0 s for the bleaching process and 4.1 s for the coloring process, respectively, which is relatively short for TPA-based electrochromic polymers.[1,6] This result can be attributed to the microscopic pores appeared in the film (Fig. S2†), which would be helpful in improving the Li^+ ions inserted/extracted efficiency and decreasing the equilibration time.

The coloration efficiency (CE) of the polymer DATPFMA was calculated from the slope of the optical density *vs.* charge density curve in the linear region (Fig. 4d). The calculated CE of the polymer film were 82.2 and 175.3 cm^2 C^{-1} in the visible and NIR regions, respectively, which suggests that the polymer film exhibits large optical modulation with small charge insertion. This result can be attributed to the specific surface morphology of the film (as shown in Fig. S2†), which is conducive to Li^+ ion insertion into the TPA groups.

Self-healing properties

The mixture of DATPF and MA turns viscous on cooling and immobile at room temperature, which indicates the formation

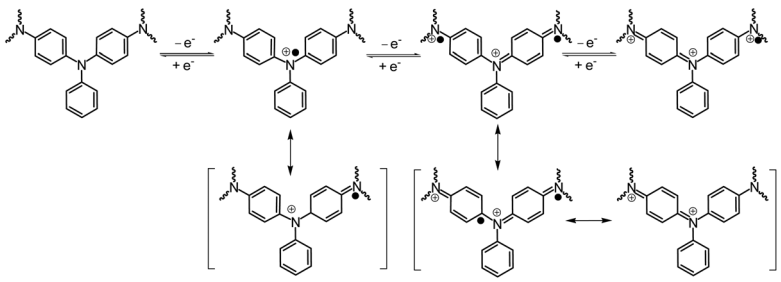

Scheme 2 Postulated redox behavior of the polymer DATPF.

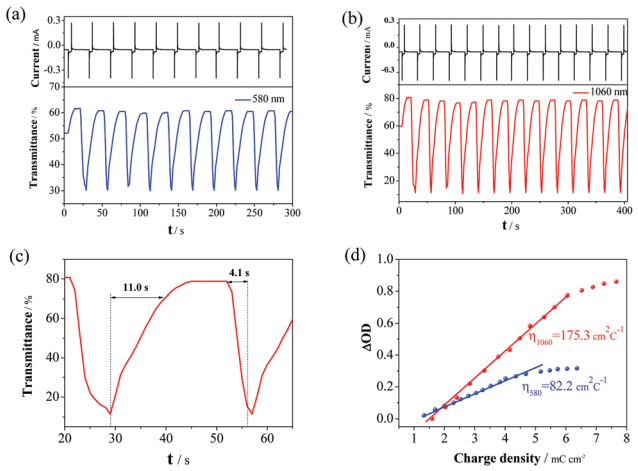

Fig. 4 Electrochromic switching response of the polymer DATPFMA film. (a) and (b) *In situ* transmittance curves change at 580 and 1060 nm and chronoamperometry curves. (c) Electrochromic switching response time. (d) Variation of the optical density (OD) at 580 and 1060 nm *versus* charge density (Q_d).

of DA bonds yielding the large molecular polymer DATPFMA (Fig. 5a). On thermal treatment at 110 °C for an hour, the viscosity of the polymer decreased proportionally with increasing temperature and then reached a flowable fluid state, which indicates the breakage of DA bonds between DATPF and MA molecules (Fig. 5b). Similarly, on cooling to room temperature once again, the DATPFMA polymer regained its original viscous state due to the reformation of DA bonds (Fig. 5c).

The invertible cleavage and formation of DA bonds indicates the self-healing properties of the polymer DATPFMA (Fig. 6). The self-healing performance is evaluated by the DA bond healing rate and measured by using the DSC enthalpy values.

The original DATPFMA (DA0) was thermally treated between temperatures 40 and 180 °C and then maintained at a constant temperature of 60 °C for 6 hours which yielded the polymer DA1 (in the procedure, the DA bond was broken and then reconstructed). The same procedure was repeated to obtain the DA2 state from the DA1 state. During this process, DA bonds were broken and then reconstructed which resulted in the formation of DA1 and then DA2 from DA0 as shown in Fig. S5.† The DA bond healing rates (η_{DSC}) were calculated by

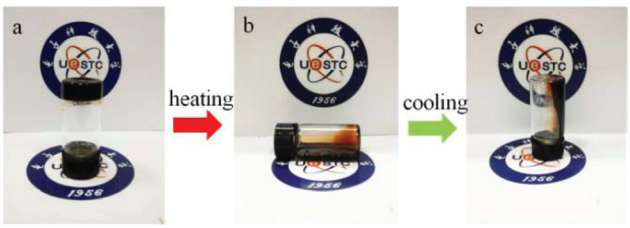

Fig. 5 The pictures of polymer DATPFMA in cyclopentanone solution at different temperatures. The state of (a) room temperature, (b) 110 °C heating for 1 h, and (c) cooling to room temperature.

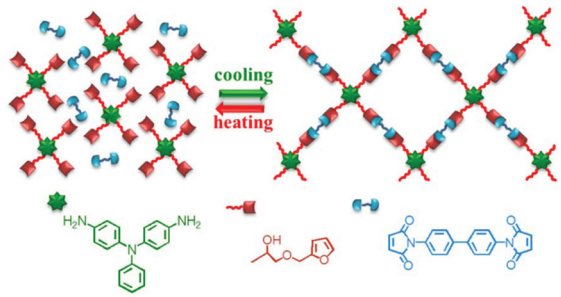

Fig. 6 Representation of the self-healing mechanism of the DATPFMA film.

the ratio of the enthalpy value of the original DATPFMA polymer (DA0) and the healed samples (DA1 and DA2); the mathematical relationship[25] can be obtained by using eqn (1):

$$\eta_{DSC} = \frac{\Delta H_{healed}}{\Delta H_{pristine}} \times 100\% \quad (1)$$

The enthalpy value (ΔH) of the endothermic peak is integrated and presented in Fig. 7a, and other DSC data are listed in Table 2. Compared with the polymer DATPFMA (DA0), the self-healing rates of the polymers DA1 and DA2 were 83% and 79%, respectively. Compared with the self-healing material based DA systems,[26] the self-healing rate of the polymer DATPFMA was higher exhibiting a great capacity for self-healing.

Fig. 7b depicts the thermal behavior of the polymer DATPFMA, which was measured between 40–200 °C by repeated DSC cycles. The negligible difference between the cycles indicates the obvious endothermic and gentle exothermic transitions in the range of 110–160 °C during successive thermal cycles. The endothermic and exothermic transitions of the polymer DATPFMA can be predominately attributed to the retro-DA and DA reactions, respectively. The slight devi-

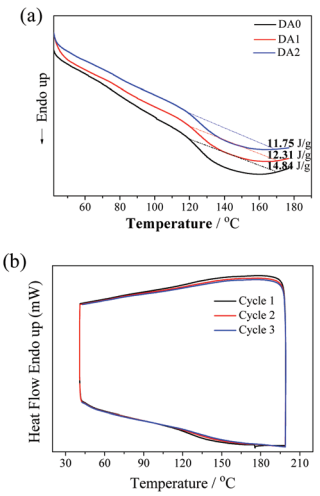

Fig. 7 (a) DSC heating traces of the self-healing sample DA0-2. (b) Repeated DSC curves of the polymer DATPFMA.

Table 2 Reaction enthalpy of polymer DATPFMA samples extracted from DSC data

Sample	Integral onset temperature (°C)	Peak temperature (°C)	Enthalpy (J g^{-1}, from 120 to 170 °C)	η_{DSC} (%)
DA0	120.92	136.58	14.84	—
DA1	120.45	136.52	12.31	83
DA2	120.91	134.74	11.75	79

ations from the repeated DSC traces in the 2nd and 3rd cycles can be attributed to the incomplete reconstruction of DA bonds with a relatively short period of DSC test time. In short, the above results clearly demonstrate that DATPFMA could be used as a thermal self-healing material.[27]

In order to further investigate the self-healing behavior, the polymer film (bleached state) was scratched with a razor blade (about 10 μm wide cuts), and the healing process at 110 °C was observed by optical microscopy, as shown in Fig. 8a–d. The scratched region starts healing with the polymer fusion and flows in the first 1 min, the scratch was gradually healed and blurred after 3 min, whereas no subsequent noticeable change was observed after 5 min. The self-healing process of the polymer DATPFMA was relatively faster compared with other polymer based DA systems,[28] which was recorded as a movie and provided in the ESI.†

Fig. 8e–h depict the electrochromic and self-healing behavior of the DATPFMA film. It is clear that at an applied voltage of 0.7 V, the color of the film varies from faint yellow to dark blue. Similarly, as discussed earlier when the film was scratched and heated at 110 °C, the scratched region regained its original condition except the color variation from dark to faint blue. The variation in the color of the polymer film from dark blue to faint blue can be explained[29] as that with the increasing of temperature, the excited electrons of the colored polymer escaped from the valence band resulting in a change of energy gap. Meanwhile, the energy barrier against the propeller-like steric geometry of triphenylamine is overcome, the frequency of the absorbed light shifted with the propeller-like steric geometry is gradually changed at the same time. From the above results, it could be seen that the self-healing process of the colored state of the polymer film was the same as the original state, in other words, the chromatic state has no influence on the self-healing process.

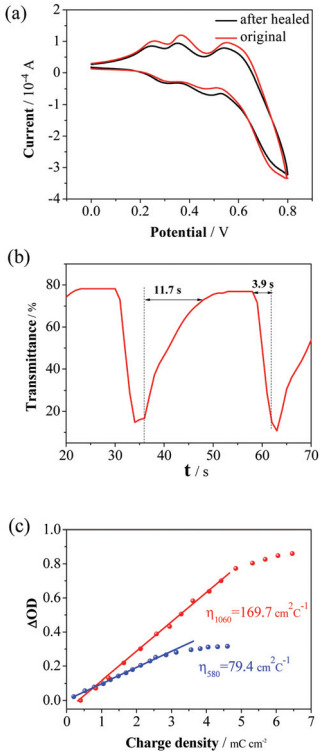

Fig. 9 Polymer DATPFMA after self-healing: (a) the CV curves of the polymer DATPFMA film before and after the self-healing process, (b) electrochromic switching response time, and (c) coloration efficiency.

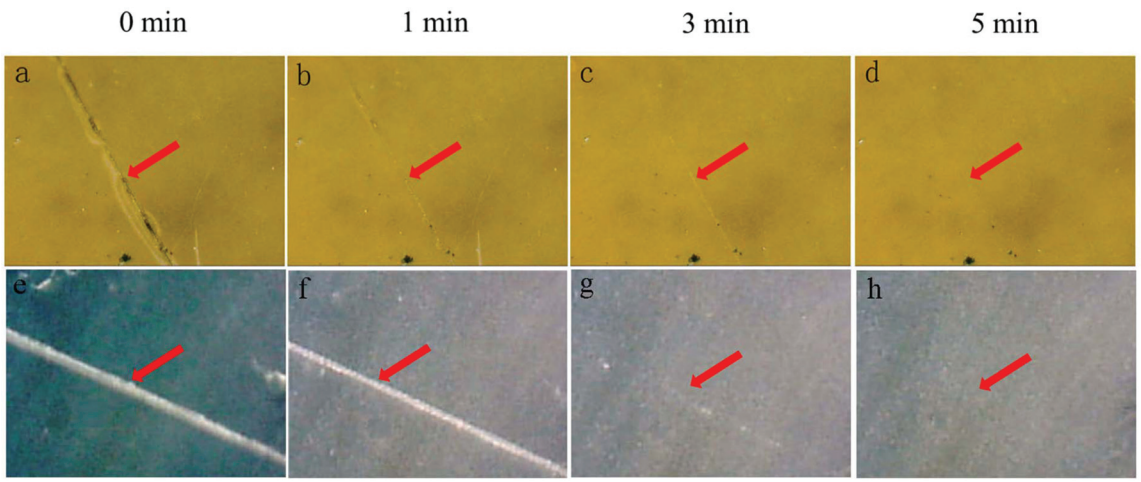

Fig. 8 Self-healing behavior of the scratched polymer DATPFMA film: (a)–(d) in the original state and (e)–(h) in the colored state.

Finally, in order to analyze the effect of self-healing, the electrochromic properties of the polymer DATPFMA films were once again investigated after self-healing at 110 °C for 5 min. The cyclic voltammetry curve of the healed film was obtained under the same conditions as the original polymer film, and the redox peaks and the area of the cyclic voltammetry curves are similar (Fig. 9a). And the colors of the healed DATPFMA film also changed from faint yellow to green grey to dark blue, the response time was 11.7 s for the bleaching process and 3.9 s for coloring (Fig. 9b), and the CEs of the polymer film after self-healing were 79.4 and 169.7 cm^2 C^{-1} in the visible and NIR regions, respectively (Fig. 9c). These results indicate that the healed polymer DATPFMA film still maintains the electrochromic properties. Briefly, the polymer DATPFMA has bisfunctions without a mutual influence of electrochromism and self-healing, which is due to the triphenylamine group and the DA group is relatively independent in the molecular structure.

Conclusion

In this paper, the TPA derivative was induced into furfuryl glycidyl ether, and further by a DA cross-linking polymerization reaction with MA to obtain a new unconjugated polymer DATPFMA with bisfunctions of electrochromism and self-healing properties. The color of the polymer film can be switched from faint yellow to green grey to dark blue, the coloring response time was 4.1 s and the bleaching response time was 11.0 s, and its coloration efficiencies were 82.2 and 175.3 cm^2 C^{-1} at 580 and 1060 nm, respectively. Meanwhile, the self-healing rate was evaluated by using the enthalpy values (ΔH) from the DSC curves with the self-healing rate at about 80%. The scratch of the polymer film can be self-healed under 110 °C during the heating process, which shows that the DATPFMA polymer has great thermal remediable and recyclable performance. All the results indicate that the polymer film with electrochromic and self-healing properties can be a promising material to overcome the scar generation in ECDs.

Conflicts of interest

There are no conficts to declare.

Acknowledgements

The authors are thankful to the National Natural Science Foundation of China (Grant No. 51773027, 21572030 and 21402023) for financial support.

References

1 R. J. Mortimer, *Annu. Rev. Mater. Res.*, 2011, **41**, 241–268.
2 J. Z. Ou, S. Balendhran, M. R. Field, D. G. McCulloch, A. S. Zoolfakar, R. A. Rani, S. Zhuiykov, A. P. O'Mullane and K. Kalantar-Zadeh, *Nanoscale*, 2012, **4**, 5980–5988.
3 B. Gadgil, P. Damlin, M. Heinonen and C. Kvarnström, *Carbon*, 2015, **89**, 53–62.
4 (*a*) A. M. Osterholm, D. E. Shen, J. A. Kerszulis, R. H. Bulloch, M. Kuepfert, A. L. Dyer and J. R. Reynolds, *ACS Appl. Mater. Interfaces*, 2015, **7**, 1413–1421; (*b*) S. L. José, R. Gómez, E. Reinold and P. Bäuerie, *Org. Lett.*, 2005, **7**, 2345–2348.
5 G. Gunbas and L. Toppare, *Chem. Commun.*, 2012, **48**, 1083–1101.
6 P. M. Beaujuge and J. Reynolds, *Chem. Rev.*, 2010, **110**, 268–320.
7 L. T. Huang, H. J. Yen and G. S. Liou, *Macromolecules*, 2011, **44**, 9595–9610.
8 (*a*) P. Zhou, Z. Wan, Y. Liu, C. Jia, X. Weng, J. Xie and L. Deng, *Electrochim. Acta*, 2016, **190**, 1015–1024; (*b*) S. Y. Kao, Y. S. Lin, C. W. Hu, M. K. Leung and K. C. Ho, *Sol. Energy Mater. Sol. Cells*, 2015, **143**, 174–182.
9 (*a*) J. J. Armao, Y. Domoto, T. Umehara, M. Maaloum, C. Contal, G. Fuks, E. Moulin, G. Decher, N. Javahiraly and N. Giuseppone, *ACS Nano*, 2016, **10**, 2082–2090; (*b*) H. J. Yen, H. Y. Lin and G. S. Liou, *Chem. Mater.*, 2011, **23**, 1874–1882.
10 P. Shi, C. M. Amb, E. P. Knott, E. J. Thompson, D. Y. Liu, J. Mei, A. L. Dyer and J. R. Reynolds, *Adv. Mater.*, 2010, **22**, 4949–4953.
11 W. Weng, T. Higuchi, M. Suzuki, T. Fukuoka, T. Shimomura, M. Ono, L. Radhakrishnan, H. Wang, N. Suzuki, H. Oveisi and Y. Yamauchi, *Angew. Chem., Int. Ed.*, 2010, **49**, 3956–3959.
12 Y. Wei, J. Zhou, J. Zheng and C. Xu, *Electrochim. Acta*, 2015, **166**, 277–284.
13 G. Cai, M. Cui, V. Kumar, P. Darmawan, J. Wang, X. Wang, A. L. Eh, K. Qian and P. S. Lee, *Chem. Sci.*, 2016, **7**, 1373–1382.
14 X. Chen, H. Lin, J. Deng, Y. Zhang, X. Sun, P. Chen, X. Fang, Z. Zhang, G. Guan and H. Peng, *Adv. Mater.*, 2014, **26**, 8126–8132.
15 C. Yan, W. Kang, J. Wang, M. Cui, X. Wang, C. Y. Foo, K. J. Chee and P. S. Lee, *ACS Nano*, 2014, **8**, 316–322.
16 (*a*) Y. Yang and M. W. Urban, *Chem. Soc. Rev.*, 2013, **42**, 7446–7467; (*b*) B. J. Blaiszik, S. L. B. Kramer, S. C. Olugebefola, J. S. Moore, N. R. Sottos and S. R. White, *Annu. Rev. Mater. Res.*, 2010, **40**, 179–211.
17 J. Li, S. Qi, J. Liang, L. Li, Y. Xiong, W. Hu and Q. Pei, *ACS Appl. Mater. Interfaces*, 2015, **7**, 14140–14149.
18 (*a*) D. H. Lee, G. Heo, K. Pyo, Y. Kim and J.-W. Kim, *ACS Appl. Mater. Interfaces*, 2016, **8**, 8129–8136; (*b*) J. Liang, L. Li, X. Niu, Z. Yu and Q. Pei, *Nat. Photonics*, 2013, **7**, 817–824.
19 (*a*) Y. Huang, M. Zhong, Y. Huang, M. Zhu, Z. Pei, Z. Wang, Q. Xue, X. Xie and C. Zhi, *Nat. Commun.*, 2015, **6**, 10310; (*b*) H. Sun, X. You, Y. Jiang, G. Guan, X. Fang, J. Deng, P. Chen, Y. Luo and H. Peng, *Angew. Chem., Int. Ed.*, 2014, **53**, 9526–9531.

20 (*a*) G. Gattuso, G. Grasso, N. Marino, A. Notti, A. Pappalardo, S. Pappalardo and M. F. Parisi, *Eur. J. Org. Chem.*, 2011, 5696–5703; (*b*) S. H. Cheng, S. H. Hsiao, T. H. Su and G. S. Liou, *Macromolecules*, 2005, **38**, 307–316.
21 E. Dolci, G. Michaud, F. Simon, B. Boutevin, S. Fouquay and S. Caillol, *Polym. Chem.*, 2015, **6**, 7851–7861.
22 J. Li, G. Zhang, L. Deng, K. Jiang, S. Zhao, Y. Gao, R. Sun and C. Wong, *J. Appl. Polym. Sci.*, 2015, **132**, 42167.
23 J. J. T. Armao, P. Rabu, E. Moulin and N. Giuseppone, *Nano Lett.*, 2016, **16**, 2800–2805.
24 (*a*) P.-I. Wang, W.-R. Shie, J.-C. Jiang, L.-J. Li and D.-J. Liaw, *Polym. Chem.*, 2016, **7**, 1505–1516; (*b*) H. Niu, H. Kang, J. Cai, C. Wang, X. Bai and W. Wang, *Polym. Chem.*, 2011, **2**, 2804–2817.
25 (*a*) G. B. Lyon, A. Baranek and C. N. Bowman, *Adv. Funct. Mater.*, 2016, **26**, 1477–1485; (*b*) J. Kötteritzsch, S. Stumpf, S. Hoeppener, J. Vitz, M. D. Hager and U. S. Schubert, *Macromol. Chem. Phys.*, 2013, **214**, 1636–1649.
26 (*a*) X. Chen, M. A. Dam, K. Ono, A. Mal, H. Shen, S. R. Nutt, K. Sheran and F. Wudl, *Science*, 2002, **295**, 1698–1702; (*b*) Y. Heo, M. H. Malakooti and H. A. Sodano, *J. Mater. Chem. A*, 2016, **4**, 17403–17411.
27 (*a*) M. Watanabe and N. Yoshie, *Polymer*, 2006, **47**, 4946–4952; (*b*) J. Li, G. Zhang, L. Deng, K. Jiang, S. Zhao, Y. Gao, R. Sun and C. Wong, *J. Appl. Polym. Sci.*, 2015, **132**, 42167.
28 (*a*) D. H. Lee, G. Heo, K. Pyo, Y. Kim and J.-W. Kim, *ACS Appl. Mater. Interfaces*, 2016, **8**, 8129–8136; (*b*) Q. Tian, Y. Yuan, M. Rong and M. Zhang, *J. Mater. Chem.*, 2009, **19**, 1289–1296.
29 (*a*) K. Yoshino, S. Nakajima, D. H. Park and R. Sugimoto, *Jpn J. Appl. Phys.*, 1988, **27**, 716–718; (*b*) C. Roux and M. Leclerc, *Macromol. Symp.*, 1994, **87**, 1–4.